

Visible-light-induced release of CO by thiolate iron(III) carbonyl complexes bearing N,C,S-pincer ligands

Toyotaka Nakae,^a Masakazu Hirotsu,^{*a} Shigetoshi Aono^b and Hiroshi Nakajima^a

^a *Division of Molecular Materials Science, Graduate School of Science, Osaka City University, 3-3-138 Sugimoto, Sumiyoshi-ku, Osaka 558-8585, Japan*

^b *Okazaki Institute for Integrative Bioscience and Institute for Molecular Science, National Institutes of Natural Sciences, 5-1 Higashiyama, Myodaiji, Okazaki, Aichi 444-8787, Japan.*

* Corresponding Author, E-mail: mhiro@sci.osaka-cu.ac.jp

Supplementary Information

Experimental section, ESR spectra of [1]PF₆ and [5]PF₆, UV-Vis-NIR spectra of [2]PF₆–[4]PF₆, ESI-mass spectra of [1]PF₆ during visible-light irradiation, UV-vis spectral change of [2]PF₆–[4]PF₆ during visible-light irradiation, electrochemical data for [1]PF₆ and [5]PF₆, ¹H and ³¹P{¹H} NMR spectra for the one-electron reduced species of [5]PF₆, crystallographic data for [1]PF₆ and [3]PF₆ and computational results are presented as supplementary information.

Experimental Section

General Procedures. All manipulations were performed under ambient atmosphere unless otherwise stated. Solvents were purchased from Kanto Chemical Co., Inc. Cobaltocene was purchased from Aldrich and used as received. Iron(II) complexes *trans*-[Fe(Lⁿ-κ³N,C,S)(CO)(PMe₂Ph)₂] (**1**, *n* = 1; **2**, *n* = 2; **3**, *n* = 3; **4**, *n* = 4)^{1,2} and tris(4-tolyl)aminium hexafluorophosphate³ were prepared according to a literature procedure. Measurement of magnetic susceptibility was carried out at 20 °C on a magnetic susceptibility balance (MSB-MKI, Sherwood Scientific Ltd.). ESR spectra were recorded on a Bruker Biospin Elexsys E500 spectrometer at room temperature. NMR spectra were recorded on a Bruker AVANCE 300 FT-NMR spectrometer at room temperature. IR spectra were recorded on a Shimadzu FTIR-8600PC by the KBr pellet method. Electronic absorption spectra were recorded on a JASCO V-570 or a Shimadzu MultiSpec-1500 spectrophotometer. Electrospray ionization mass spectrometry was performed on an Applied Biosystem Mariner time-of-flight mass spectrometer. Elemental analyses were performed by the Analytical Research Service Center at Osaka City University on J-SCIENCE LAB JM10 or FISIONS Instrument EA1108 elemental analyzers. Photolysis was carried out using a white LED (Hayashi watch works Co., Ltd., LA-158AS).

Preparation of *trans*-[Fe(L¹-κ³N,C,S)(CO)(PMe₂Ph)₂]PF₆ ([1**]PF₆).** To a solution of **1** (180 mg, 0.29 mmol) in dichloromethane (3 mL), tris(4-tolyl)aminium hexafluorophosphate (131 mg, 0.30 mmol) in dichloromethane (2 mL) was added in the dark. The reaction solution was stirred at room temperature for 10 minutes, and then the solvent was removed under reduced pressure. To the residual dark green oil, diethyl ether (2 mL) was added and stirred for 10 min to afford a dark green precipitate. The precipitate was collected by filtration, washed with diethyl ether, and dried under reduced pressure. The title complex was obtained as a dark green powder (199 mg, 90%). Suitable single crystals for X-ray diffraction analysis were obtained by vapor diffusion of diethyl ether into a THF solution of [**1**]PF₆ in the dark. IR (KBr): ν_{CO}/cm⁻¹ 1890. Anal. Calcd for C₃₄H₃₃F₆FeNOP₃S·0.33H₂O: C, 52.87; H, 4.39; N, 1.81. Found: C, 52.87; H, 4.47; N, 1.90.

Preparation of *trans*-[Fe(L²-κ³N,C,S)(CO)(PMe₂Ph)₂]PF₆ ([2**]PF₆).** To a solution of **2** (32.1 mg, 0.050 mmol) in dichloromethane (4 mL), tris(4-tolyl)aminium hexafluorophosphate (26.1 mg, 0.060 mmol) in dichloromethane (6 mL) was added in the dark. The reaction solution was stirred at room temperature for 10 minutes, and then

the solvent was removed under reduced pressure. To the residual dark green oil, diethyl ether (2 mL) was added and stirred for 10 min to afford a dark green precipitate. The precipitate was collected by decantation, washed with diethyl ether, and dried under reduced pressure to give a dark green powder of [2]PF₆ (38.3 mg, 97%). IR (KBr): $\nu_{\text{CO}}/\text{cm}^{-1}$ 1963. Anal. Calcd for C₃₄H₃₄F₆FeN₂OP₃S·0.75CH₂Cl₂: C, 49.38; H, 4.23; N, 3.31. Found: C, 49.38; H, 4.27; N, 3.52.

Preparation of *trans*-[Fe(L³- κ^3 N,C,S)(CO)(PMe₂Ph)₂]PF₆ ([3]PF₆). Complex 3 (63.5 mg, 0.10 mmol) and tri(4-tolyl)aminium hexafluorophosphate (46.6 mg, 0.11 mmol) were dissolved in dichloromethane (5 mL) in the dark. The reaction mixture was stirred at room temperature for 5 min. The solvent was removed under reduced pressure. To the dark green residue, diethyl ether (2 mL) was added and stirred for 10 min, to afford a dark green precipitate. The precipitate was collected by decantation, washed with diethyl ether, and dried under reduced pressure to give a dark green powder of [3]PF₆ (70.8 mg, 91%). Suitable single crystals for X-ray diffraction analysis were obtained by vapor diffusion of diethyl ether into a THF solution of [3]PF₆ in the dark. IR(KBr), $\nu_{\text{CO}}/\text{cm}^{-1}$ 1976. Anal. Calcd for C₃₄H₃₄F₆FeN₃OP₃S: C, 52.26; H, 4.39; N, 3.58. Found: C, 52.63; H, 4.53; N, 3.55.

Preparation of *trans*-[Fe(L⁴- κ^3 N,C,S)(CO)(PMe₂Ph)₂]PF₆ ([4]PF₆). Complex 4 (63.4 mg, 0.10 mmol) and tri(4-tolyl)aminium hexafluorophosphate (45.3 mg, 0.10 mmol) were dissolved in dichloromethane (7 mL) in the dark. The reaction mixture was stirred at room temperature for 5 min. The solvent was removed under reduced pressure. To the dark green residue, diethyl ether (2 mL) was added and stirred for 10 min, and then dark green solid was separated by decantation. The residual dark green powder was washed with diethyl ether 3 times. The residual solid was dried under reduced pressure to give a dark green powder of [4]PF₆ (75.7 mg, 97%). IR(KBr) $\nu_{\text{CO}}/\text{cm}^{-1}$ 1983. Anal. Calcd for C₃₄H₃₄F₆FeN₃OP₃S: C, 52.26; H, 4.39; N, 3.58. Found: C, 52.50; H, 4.46; N, 3.68.

Synthesis of *trans*-[Fe(PyBPT)(CN^tBu)(PMe₂Ph)₂]PF₆ ([5]PF₆). To a solution of [1]PF₆ (30.0 mg, 0.039 mmol) in dichloromethane (5 mL) was added *tert*-butyl isocyanide (13.5 μ L, 0.13 mmol). The dark green solution was irradiated in an ice bath for 5 h with a white LED. The resulting dark brown solution was evaporated under reduced pressure. The gummy residue was dissolved in a small amount of dichloromethane, and then *n*-hexane was slowly added. A dark brown powder was precipitated, collected by filtration, and washed with *n*-hexane (27.1 mg, 84%). IR

(KBr): $\nu_{\text{CN}}/\text{cm}^{-1}$ 2132. ESI-MS m/z 676. Anal. Calcd for $\text{C}_{38}\text{H}_{42}\text{F}_6\text{FeN}_2\text{P}_3\text{S}$: C, 55.55; H, 5.15; N, 3.41. Found: C, 55.41; H, 5.30; N, 3.65.

Reduction of [5]PF₆. Reduction of [5]PF₆ was performed using a glovebox under an atmosphere of oxygen-free dry nitrogen. To a solution of [5]PF₆ (9.2 mg, 11 μmol) in THF (1 mL) was added cobaltocene (2.9 mg, 15 μmol). The reaction mixture was stirred for 5 min, and the solvent was removed under reduced pressure. *n*-Hexane (5 mL) was added to the dark red brown residue. The suspension was passed through Celite pad, and the filtrate was evaporated to dryness. The resulting red brown powder (5 mg) was dissolved in C_6D_6 , and ^1H and $^{31}\text{P}\{^1\text{H}\}$ NMR spectra of the solution were measured. ^1H NMR (300 MHz, C_6D_6): δ 0.87 (dd, $^2J_{\text{PH}} = ^4J_{\text{PH}} = 3.6$ Hz, 6H, PMe_2Ph), 1.23 (s, 9H, CN^tBu) 1.61 (dd, $^2J_{\text{PH}} = ^4J_{\text{PH}} = 3.6$ Hz, 6H, PMe_2Ph), 5.72 (ddd, $^3J_{\text{HH}} = 5.8$, 7.2 Hz, $^4J_{\text{HH}} = 1.4$ Hz, 1H), 6.47 (ddd, $^3J_{\text{HH}} = 7.2$, 8.1 Hz, $^4J_{\text{HH}} = 1.4$ Hz, 1H), 6.73–6.91 (m, 11H), 6.99 (ddd, $^3J_{\text{HH}} = 6.9$, 7.7 Hz $^4J_{\text{HH}} = 1.6$ Hz, 1H, 5-py), 7.07 (ddd, $^3J_{\text{HH}} = 6.9$, 7.9 Hz, $^4J_{\text{HH}} = 1.6$ Hz, 1H, 4-Py) 7.35 (tt, $^3J_{\text{HH}} = 7.6$ Hz, $J_{\text{PH}} = 1.6$ Hz, 1H, 5'-BPT), 7.46 (dd, $^3J_{\text{HH}} = 7.6$ Hz, $^4J_{\text{HH}} = 1.1$ Hz, 1H), 7.90–7.97 (m, 2H), 8.13 (d, $^3J_{\text{HH}} = 7.7$ Hz, 1H, 3-Py), 8.23 (d, $^3J_{\text{HH}} = 7.7$ Hz, $^4J_{\text{HH}} = 1.6$ Hz 1H, 6-Py). $^{31}\text{P}\{^1\text{H}\}$ NMR (121.5 MHz, C_6D_6): δ 30.2 (s).

Photochemistry. The quantum yield for CO-elimination reaction of [1]PF₆ was determined at 405 nm with a 10 nm bandwidth using a built-in xenon lamp of a Hitachi F-7000 fluorescence spectrophotometer as a light source. Dichloromethane solutions of [1]PF₆ were used for the quantum-yield determination because the product is readily decomposed in acetonitrile, and the reactions were performed in the presence of 1,10-phenanthroline in order to avoid precipitation of decomposed iron species. The decrease of the reactant concentration was quantitated by absorption at 860 nm as a function of irradiation time. Potassium tris(oxalato)ferrate(III) trihydrate was used as an actinometer to determine the intensity of the light.

Electrochemistry. Cyclic voltammetric measurements were performed at room temperature with an ALS/CHI600A voltammetric analyzer (Bioanalytical System Ins.) under N_2 . Cyclic voltammograms of [1]PF₆ and [5]PF₆ are shown in Fig. S7, and electrochemical data are summarized in Table S1. Working, reference, and counter electrodes were a glassy carbon disk electrode with a diameter of 3 mm, a Ag/Ag^+ (0.010 M AgNO_3 , 1 M = 1 mol dm^{-3}) reference electrode, and a platinum wire, respectively. Sample solutions were prepared in the concentration of 0.50 mM

containing 0.10 M Bu₄NPF₆ as a supporting electrolyte. The electrode potentials were corrected using the redox potential of ferrocenium/ferrocene (Fc⁺/Fc) obtained under the same conditions. The sample solutions were degassed using N₂ prior to each measurement.

X-ray Crystal Structure Determination of [1]PF₆ and [3]PF₆. Diffraction data of [1]PF₆ and [3]PF₆ were collected on a Rigaku AFC11/Saturn 724+ CCD diffractometer. The data were processed and corrected for Lorentz and polarization effects using the CrystalClear software package.⁴ The analyses were carried out using the WinGX software.⁵ Absorption corrections were applied using the Multi Scan method. The structures were solved using direct methods (SIR97⁶) and refined by full-matrix least-squares on F^2 using SHELXL-2013.⁷ Crystallographic data are summarized in Tables S2. Non-hydrogen atoms were refined anisotropically. Hydrogen atoms were located in a difference Fourier map and refined isotropically.

Computational Details. The Structure of complex [1]⁺ was optimized by DFT calculations using the Gaussian 03 program package.⁸ The uB3LYP density functional method and the 6-311G(d,p) or 6-311+G(d,p) basis set were used for the calculations. The initial model was obtained from the crystal structure of [1]PF₆. Optimized structures and selected molecular orbitals of [1]⁺ are shown in Fig. S10 and S11, and its molecular coordinates are listed in Table S3. Harmonic vibrational frequencies were calculated for the optimized geometries using the 6-311G(d,p) level of theory. Time-dependent DFT calculations for [1]⁺ were performed using the optimized structures at the uB3LYP/6-311+G(d,p) level, and the calculated electronic transitions are given in Table S6.

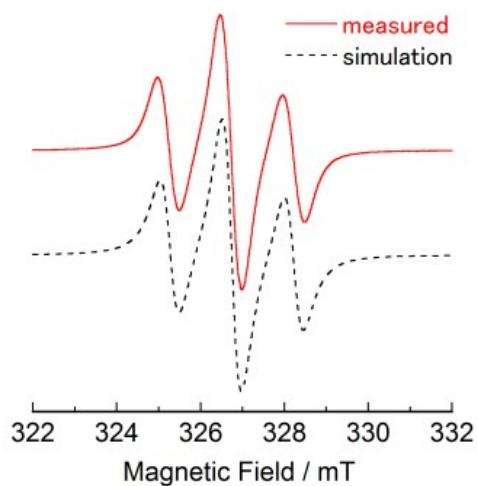


Fig. S1 Solution ESR spectrum of [1]PF₆ in butyronitrile at 20 °C. Top: Observed spectrum. Bottom: Simulation.

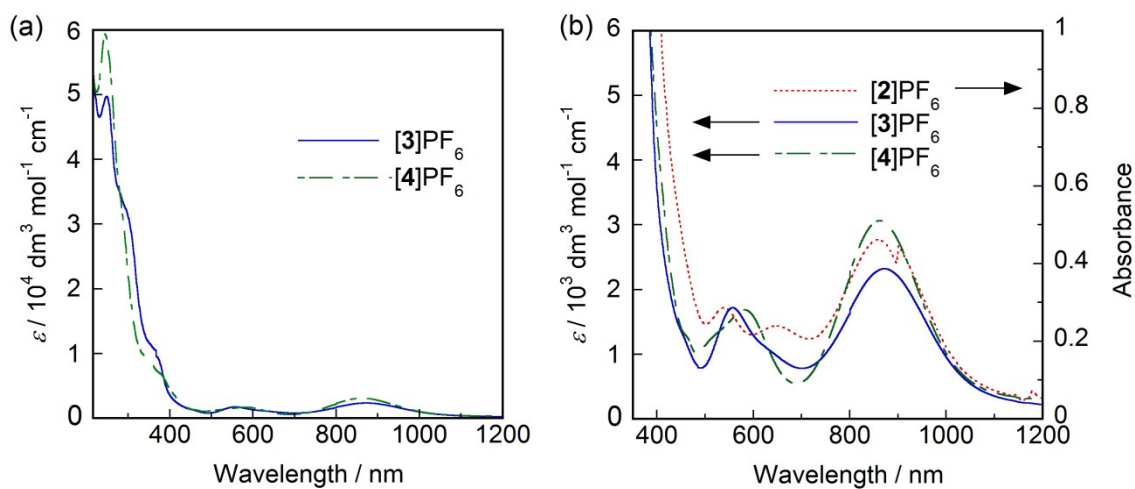


Fig. S2 (a) UV-vis-NIR spectra of [3]PF₆ and [4]PF₆ in acetonitrile. (b) Vis-NIR spectra of [2]PF₆–[4]PF₆ in acetonitrile. The molar absorption coefficient of [2]PF₆ was not determined because of the photosensitivity.

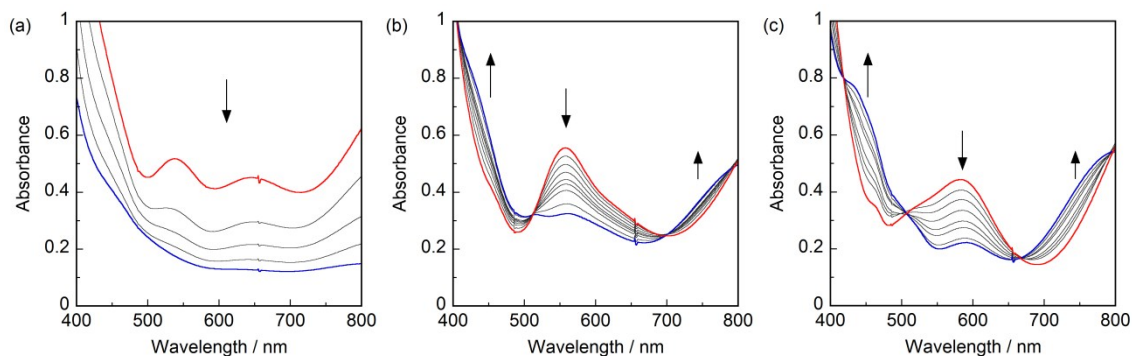


Fig. S3 Spectral changes in acetonitrile during the photoreactions of (a) $[2]PF_6$, (b) $[3]PF_6$ and (c) $[4]PF_6$ at 0 °C. The red lines show spectra before irradiation. The blue lines show spectra after 5 min irradiation.

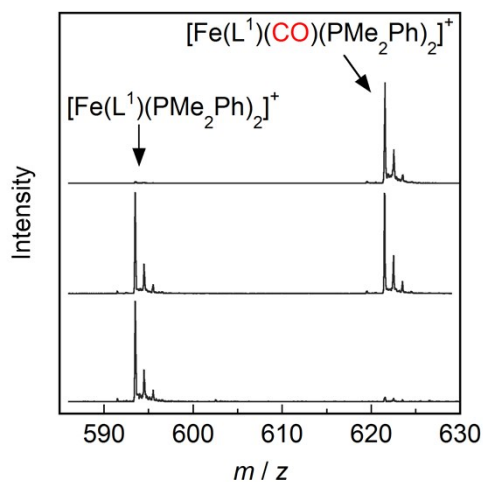


Fig. S4 ESI-Mass spectral changes in acetonitrile during the photoreaction of $[1]PF_6$. Top: Before irradiation. Middle: After 3 min irradiation. Bottom: After 9 min irradiation.

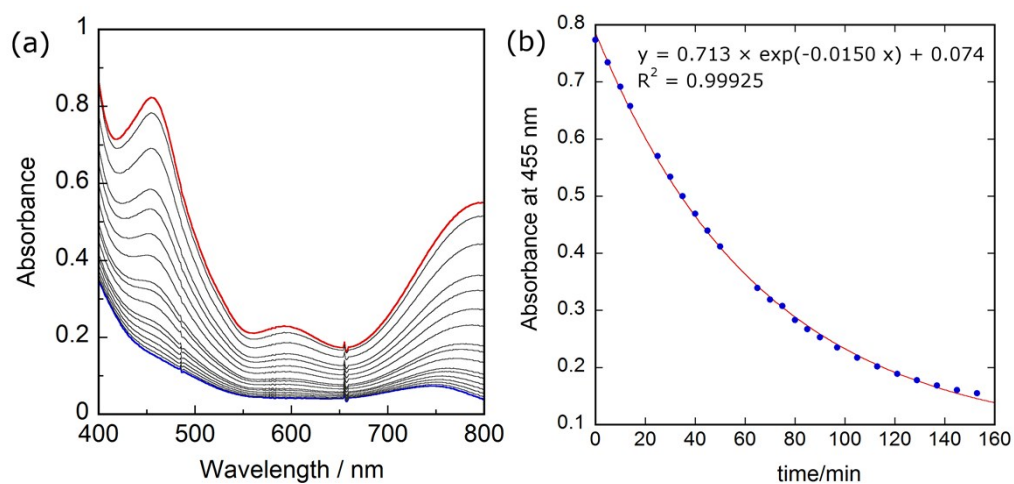


Fig. S5 (a) UV-vis spectral change of the photoreaction product of [1]PF₆ in acetonitrile at room temperature. The red line is the initial spectrum, and the blue line is the spectrum after 160 min at room temperature (17 °C). (b) A plot of the absorbance at 455 nm as a function of time. The data can be fitted by first-order exponential decay (solid line), and the fitting equation is shown in the diagram ($k = 0.0150 \text{ min}^{-1}$).

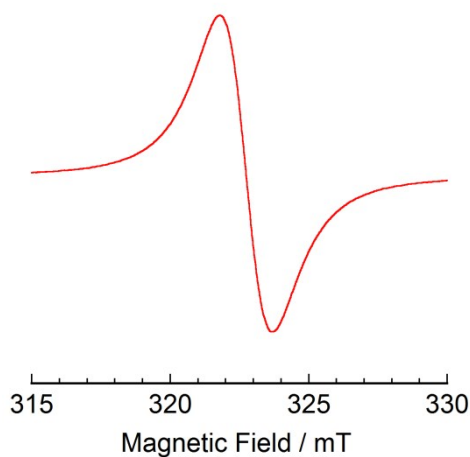


Fig. S6 Solution ESR spectrum of [5]PF₆ in butyronitrile at 20 °C. The isotropic g -value is 2.068.

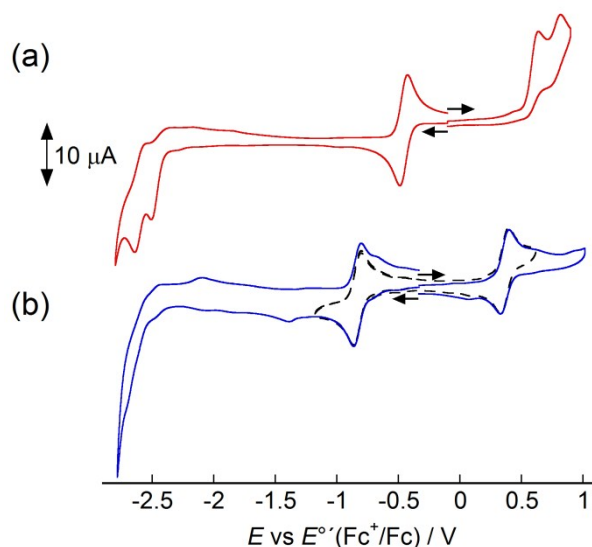


Fig. S7 Cyclic voltammograms of (a) [1]PF₆ (0.5 mM) and (b) [5]PF₆ (0.5 mM) in CH₃CN containing 0.10 M Bu₄NPF₆: scan rate, 0.1 V s⁻¹; working electrode, glassy carbon; auxiliary electrode, platinum wire; reference electrode, Ag/Ag⁺. Potentials are versus ferrocenium/ferrocene (Fc⁺/Fc).

Table S1 Electrochemical data for [1]PF₆ and [5]PF₆^a

Complex	Reduction	Oxidation
	$E_{1/2}/V(\Delta E_p/mV)^b$	$E_{1/2}/V(\Delta E_p/mV)^b$
[1]PF ₆	-0.46 (58)	0.60 (82) ^c
[5]PF ₆	-0.83 (64)	0.36 (67)

^aData from cyclic voltammetric measurements in CH₃CN with 0.10 M Bu₄NPF₆ as a supporting electrolyte; scan rate, 0.1 V s⁻¹; working electrode, glassy carbon; auxiliary electrode, platinum wire; reference electrode, Ag/Ag⁺. ^bPotentials are given vs $E^\circ(\text{Fc}^+/\text{Fc})$; ΔE_p , peak to peak separation. ^cScan rate, 1 V s⁻¹.

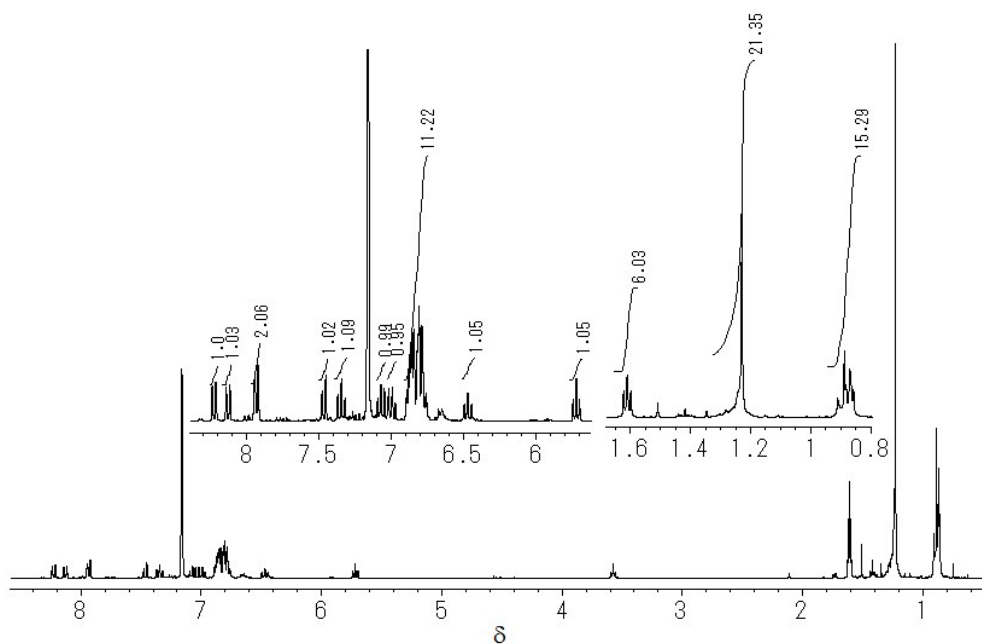


Fig. S8 ^1H NMR spectrum (300 MHz, C_6D_6) of the reduction product of $[\mathbf{5}]\text{PF}_6$. Signals of coordinated $t\text{BuNC}$ (1.23 ppm, 9H) and PMe_2Ph (0.87 ppm, 6H) overlap with those of residual n -hexane.

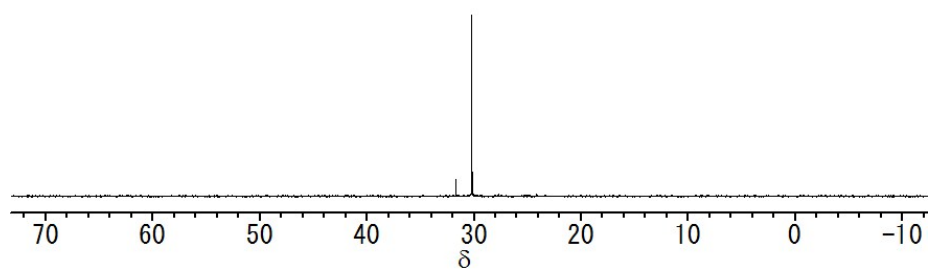


Fig. S9 $^{31}\text{P}\{^1\text{H}\}$ NMR spectrum (121 MHz, C_6D_6) of the reduction product of $[\mathbf{5}]\text{PF}_6$.

Table S2 Crystallographic data for [1]PF₆ and [3]PF₆.

	[1]PF ₆	[3]PF ₆
Empirical formula	C ₃₄ H ₃₃ F ₆ FeNO P ₃ S	C ₃₄ H ₃₄ F ₆ FeN ₂ O P ₃ S
Formula weight	766.43	781.45
Temperature/K	153	133
Wavelength/Å	0.71075	0.71075
Crystal system	monoclinic	monoclinic
Space group	<i>P</i> 2 ₁ / <i>n</i> (#14)	<i>P</i> 2 ₁ / <i>n</i> (#14)
<i>a</i> /Å	9.3243(4)	9.4165(6)
<i>b</i> /Å	30.8976(15)	31.156(2)
<i>c</i> /Å	11.4402(5)	11.4963(8)
α /°	90	90
β /°	91.022(3)	93.943(4)
γ /°	90	90
<i>V</i> /Å ³	3295.4(3)	3364.8(4)
<i>Z</i>	4	4
<i>D</i> _{calcd} /Mg m ⁻³	1.545	1.543
μ (Mo K α)/mm ⁻¹	0.731	0.719
<i>F</i> (000)	1572.00	1604.00
Crystal size/mm ³	0.21 × 0.09 × 0.03	0.23 × 0.04 × 0.02
Reflections collected	33733	34531
Independent reflections	7440 (<i>R</i> _{int} = 0.0438)	7641 (<i>R</i> _{int} = 0.0702)
Completeness to θ	0.993 (θ = 27.417°)	0.995 (θ = 27.448°)
Max. and min. transmission	1.0000 and 0.9278	1.0000 and 0.9341
No. of data/restraints/parameters	7440/0/556	7641/0/569
Goodness of fit on <i>F</i> ²	1.051	1.070
Final <i>R</i> indices [<i>I</i> > 2 σ (<i>I</i>)]	<i>R</i> ₁ = 0.0509	<i>R</i> ₁ = 0.0611
<i>R</i> indices (all data)	<i>wR</i> ₂ = 0.1247	<i>wR</i> ₂ = 0.1335
Largest diff. peak and hole (e Å ⁻³)	1.797 and -0.825	0.598 and -0.554

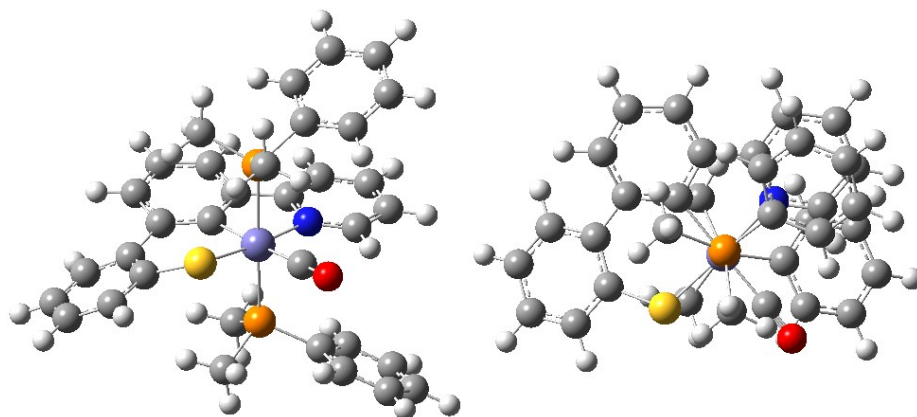
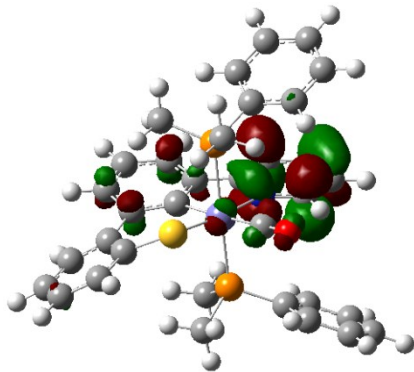
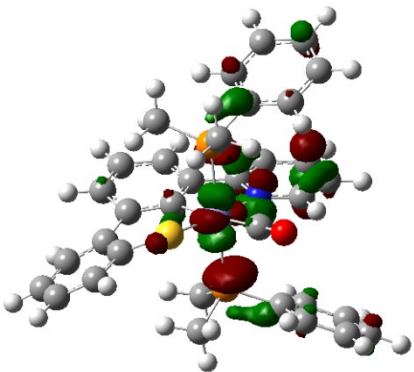
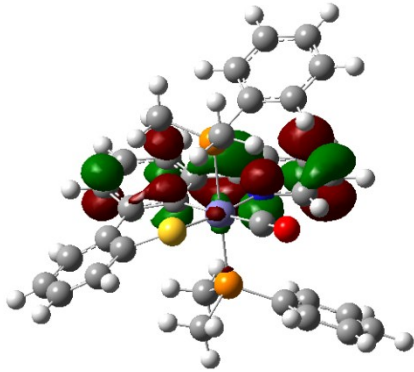
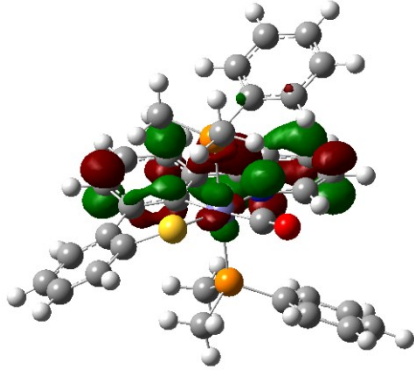
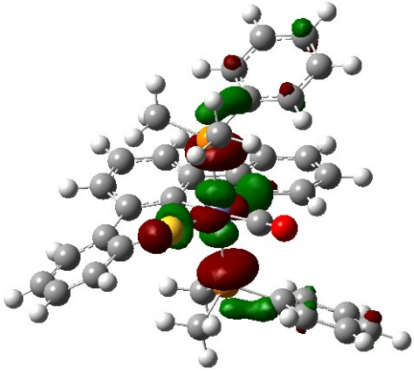
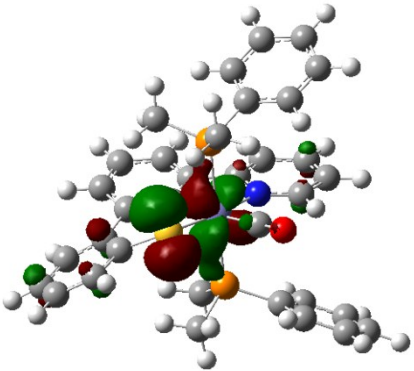
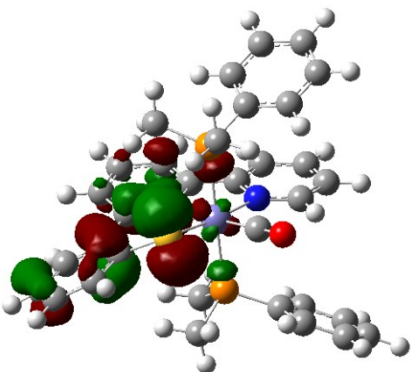
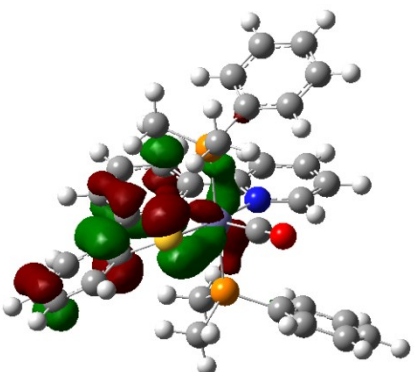
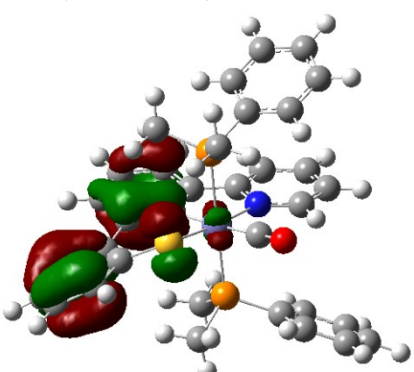
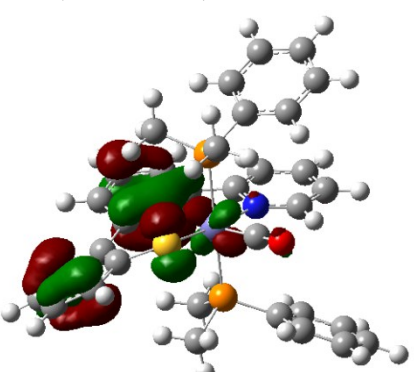
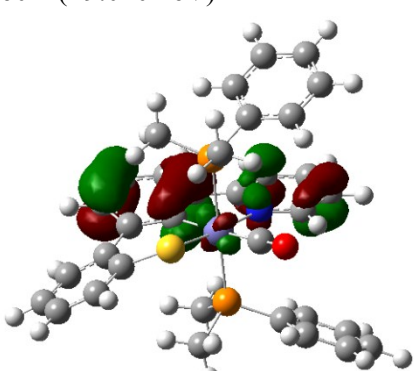
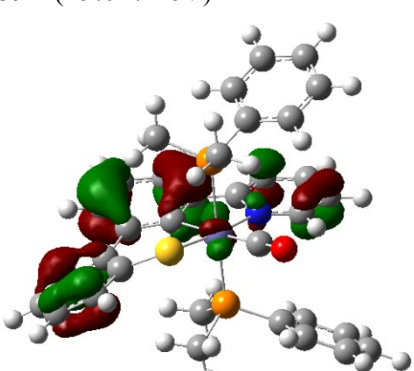


Fig. S10 Molecular structures of $[1]^+$ optimized by the DFT calculation at the uB3LYP/6-311+G(d,p) level.

	α orbitals	β orbitals
LUMO+2	165A (-4.2263 eV) 	164B (-4.4866eV) 
LUMO+1	164A (-4.6006 eV) 	163B (-4.6031eV) 

LUMO	163A (-4.9082 eV) 	162B (-5.8998 eV) 
HOMO	162A (-8.2243 eV) 	161B (-8.4431 eV) 
HOMO-1	161A (-8.8877 eV) 	160B (-8.7708 eV) 
HOMO-2	160A (-9.0101 eV) 	159B (-9.0171 eV) 

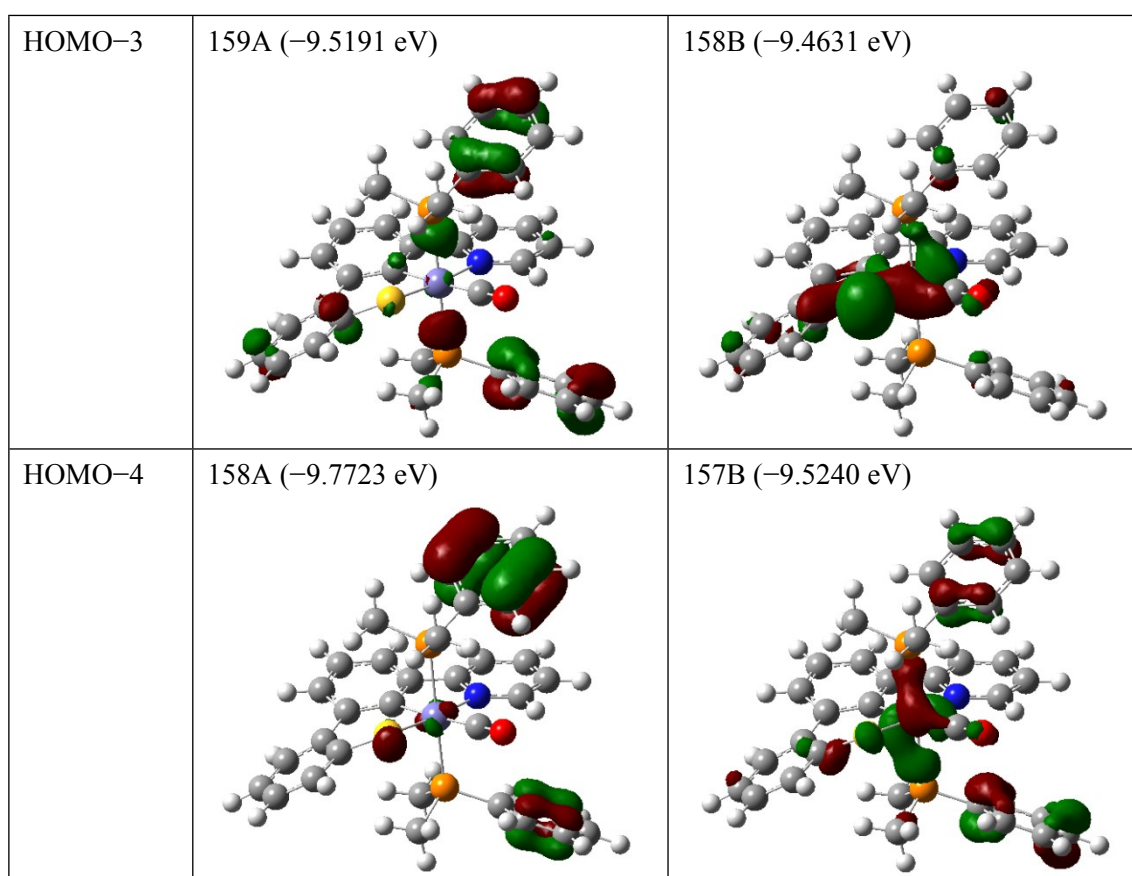


Fig. S11 Selected molecular orbitals (isovalue = 0.04) of $[1]^+$ calculated by DFT at the uB3LYP/6-311+G(d,p) level.

Table S3 Molecular coordinates of $[1]^+$ optimized by the DFT calculation at the uB3LYP/6-311+G(d,p) Level

	Atomic number	$x/\text{\AA}$	$y/\text{\AA}$	$z/\text{\AA}$
1	6	-1.68834	1.945546	2.091192
2	6	-1.07779	-2.70013	3.250565
3	6	0.077124	-1.95055	3.090397
4	6	2.432339	-0.11176	2.681393
5	6	1.29826	5.184029	1.144497
6	6	3.488998	0.730637	2.380997
7	6	0.518086	4.035745	1.271179
8	6	-2.13426	-2.52085	2.365842
9	6	0.188252	-1.09225	1.988109
10	6	1.369144	-0.25486	1.77855

11	6	1.379171	5.845894	-0.07822
12	6	-4.56393	-1.58723	1.147709
13	6	3.475655	1.434473	1.176919
14	6	-0.1977	3.537532	0.174698
15	6	-2.06901	-1.61772	1.283739
16	6	-0.84554	-0.95792	1.022293
17	6	-5.77491	-1.45217	0.482741
18	6	-2.81364	2.513403	-0.48435
19	6	-3.32159	-1.39172	0.509829
20	6	2.399643	1.260674	0.326462
21	6	0.67468	5.355823	-1.17712
22	6	-0.1063	4.209831	-1.05342
23	6	-5.78942	-1.10707	-0.86825
24	6	-3.36063	-0.9759	-0.83824
25	6	4.353808	-3.27529	0.382601
26	6	3.007404	-3.08903	0.072705
27	6	-4.58801	-0.86228	-1.51531
28	6	0.022392	-3.49158	-0.88374
29	6	5.336555	-2.56041	-0.29756
30	6	0.40556	0.952044	-2.07738
31	6	2.627929	-2.18471	-0.92766
32	6	4.968588	-1.64982	-1.28718
33	6	3.625003	-1.45835	-1.59598
34	6	0.888745	-2.08852	-3.22181
35	1	-2.07237	2.914169	2.417319
36	1	1.836195	5.563665	2.005547
37	1	-0.83495	1.662988	2.706541
38	1	2.422826	-0.65783	3.614391
39	1	0.465297	3.543635	2.234374
40	1	-1.16627	-3.40852	4.065479
41	1	0.884819	-2.05262	3.805127
42	1	4.313348	0.841686	3.07561
43	1	-2.45944	1.185392	2.214506
44	1	-4.58332	-1.83369	2.201265
45	1	-3.02898	-3.1124	2.511356
46	1	-6.70303	-1.61071	1.018984

47	1	1.981179	6.741873	-0.17393
48	1	-3.15513	3.459503	-0.05997
49	1	4.277215	2.106329	0.90016
50	1	-3.55991	1.738937	-0.30732
51	1	2.350517	1.79904	-0.61009
52	1	4.63266	-3.98896	1.14932
53	1	-2.68325	2.620146	-1.56066
54	1	2.262387	-3.66465	0.607637
55	1	-0.03705	-3.5744	0.200162
56	1	-6.72535	-1.01043	-1.40556
57	1	0.72568	5.869405	-2.13012
58	1	-0.65214	3.85534	-1.92011
59	1	6.383243	-2.71562	-0.06343
60	1	-0.99252	-3.46744	-1.28111
61	1	-4.58371	-0.56623	-2.55807
62	1	0.554391	-4.35144	-1.29549
63	1	5.727814	-1.09392	-1.82518
64	1	3.363939	-0.74978	-2.37434
65	1	-0.13578	-2.05514	-3.59402
66	1	1.452181	-1.27544	-3.6789
67	1	1.348792	-3.03756	-3.50282
68	7	1.367444	0.441855	0.610003
69	8	0.770113	1.468743	-3.02666
70	15	-1.2316	2.02031	0.31374
71	15	0.863591	-1.93911	-1.38459
72	16	-1.94583	-0.55687	-1.81621
73	26	-0.22794	0.054631	-0.58533

Table S4 Selected bond distances (Å) and angles (deg) obtained from DFT calculations at the uB3LYP/6-311+G(d,p) level and X-ray diffraction analysis (XRD)

	calculation		XRD	
	1 ¹	[1] ⁺	1 ¹	[1]PF ₆
Fe1–S1	2.3461	2.2000	2.2878(8)	2.1532(8)
Fe1–C7	2.0081	1.9978	1.986(2)	1.988(3)
Fe1–N1	2.0239	2.0308	1.990(2)	2.003(2)
Fe1–C18	1.7916	1.8528	1.760(2)	1.817(3)
Fe1–P1	2.3497	2.4094	2.2658(5)	2.3123(8)
Fe1–P2	2.3227	2.3832	2.2339(5)	2.2937(8)
C18–O1	1.1549	1.1406	1.166(3)	1.141(4)
Fe1–C18–O1	178.79	177.31	178.41(17)	175.5(3)
S1–Fe1–C18	88.14	87.19	89.22(8)	88.06(9)
N1–Fe1–C18	97.17	96.49	96.30(10)	95.81(11)
N1–Fe1–S1	173.26	174.72	173.86(6)	175.66(7)
P1–Fe1–P2	174.89	176.81	174.59(2)	174.54(3)
C7–Fe1–C18	177.93	177.72	177.98(8)	175.68(12)

Table S5 Selected Mulliken atomic spin densities of [**1**]⁺ calculated by DFT at the uB3LYP/6-311G(d,p) level

atom	spin densities
Fe1	0.963633
S1	0.195128
C7	-0.044661
N1	-0.012595
C18	-0.046892
P1	-0.042212
P2	-0.038684

Table S6 Energies of electronic transitions of [1]⁺ calculated by TD-DFT at the uB3LYP/6-311+G(d,p) level

State	Component (coefficient)	<i>E</i> /eV	<i>λ</i> /nm	<i>f</i>
1	150B -> 162B (-0.18070)	0.8495	1459.47	0.0005
	151B -> 162B (-0.27730)			
	152B -> 162B (-0.39655)			
	153B -> 162B (0.22837)			
	156B -> 162B (-0.14666)			
	157B -> 162B (0.30813)			
	158B -> 162B (0.50161)			
	158B -> 164B (0.10548)			
	159B -> 162B (-0.23839)			
	160B -> 162B (0.56066)			
2	149B -> 162B (0.10416)	0.9037	1371.91	0.0017
	150B -> 162B (0.15919)			
	151B -> 162B (0.14871)			
	152B -> 162B (-0.12353)			
	153B -> 162B (-0.35111)			
	154B -> 162B (0.10233)			
	156B -> 162B (0.26636)			
	157B -> 162B (0.50652)			
	158B -> 162B (0.47677)			
	159B -> 162B (0.16554)			
	160B -> 162B (-0.33765)			
	161B -> 162B (0.40515)			
3	155A -> 163A (0.11809)	1.3036	951.07	0.0349
	150B -> 162B (-0.10066)			
	153B -> 162B (0.16039)			
	157B -> 162B (-0.15726)			
	159B -> 162B (0.16765)			
	160B -> 162B (0.34445)			
	161B -> 162B (0.95835)			
4	149A -> 163A (0.10755)	1.9705	629.21	0.0013
	150A -> 163A (0.10142)			
	153A -> 163A (0.50293)			
	154A -> 163A (-0.11629)			

	155A -> 163A (-0.19867) 157A -> 163A (0.18132) 152B -> 163B (-0.14054) 152B -> 164B (-0.21246) 157B -> 163B (0.21901) 157B -> 164B (0.37236) 157B -> 165B (0.14824) 157B -> 170B (-0.13966) 158B -> 163B (0.24616) 158B -> 164B (0.44230) 158B -> 165B (0.16534) 158B -> 170B (-0.15375) 161B -> 163B (0.12209) 161B -> 164B (0.17891)			
5	149A -> 163A (-0.17613) 150A -> 163A (0.36033) 151A -> 163A (0.10421) 152A -> 163A (0.19865) 154A -> 163A (0.20311) 160A -> 163A (0.30025) 161A -> 163A (-0.22831) 162A -> 163A (-0.29818) 150B -> 164B (-0.15562) 151B -> 163B (-0.11670) 151B -> 164B (-0.20727) 152B -> 164B (-0.11407) 153B -> 163B (0.16588) 153B -> 164B (0.27885) 153B -> 165B (0.11041) 156B -> 163B (-0.11464) 156B -> 164B (-0.19081) 159B -> 163B (-0.10587) 159B -> 164B (-0.17865) 160B -> 163B (0.23817) 160B -> 164B (0.37875) 160B -> 165B (0.13614)	1.9961	621.12	0.0003

	161B -> 163B (-0.11651) 161B -> 164B (-0.17744)			
6	139A -> 163A (0.12883) 145A -> 163A (-0.16231) 147A -> 163A (0.15202) 149A -> 163A (0.13184) 150A -> 163A (0.11907) 151A -> 163A (0.20064) 154A -> 163A (0.16391) 157A -> 163A (0.10677) 161A -> 163A (-0.25241) 162A -> 163A (0.78918) 161B -> 164B (-0.12261)	2.1334	581.15	0.0127
7	162A -> 163A (0.13448) 149B -> 162B (-0.11342) 152B -> 162B (0.49836) 153B -> 162B (0.19604) 155B -> 162B (-0.18579) 158B -> 162B (0.48014) 159B -> 162B (0.55824) 160B -> 162B (0.14866) 161B -> 162B (-0.18233) 161B -> 164B (0.10671)	2.2165	559.37	0.0015
8	151B -> 162B (0.21110) 152B -> 162B (-0.21051) 153B -> 162B (-0.34080) 155B -> 162B (0.22786) 156B -> 162B (0.18422) 157B -> 162B (0.12426) 158B -> 162B (-0.30636) 159B -> 162B (0.48794) 160B -> 162B (0.53602) 161B -> 162B (-0.18319)	2.3066	537.52	0.0086
9	149A -> 163A (-0.10759) 153A -> 163A (-0.10299) 162A -> 163A (0.15699)	2.4713	501.69	0.0040

	146B -> 162B (-0.18200) 149B -> 162B (-0.26126) 151B -> 162B (0.29713) 152B -> 162B (0.21851) 153B -> 162B (-0.14525) 155B -> 162B (0.29203) 159B -> 162B (-0.40183) 159B -> 164B (0.13979) 160B -> 162B (0.18693) 160B -> 163B (0.13496) 160B -> 164B (0.15993) 161B -> 163B (0.34145) 161B -> 164B (0.48361) 161B -> 165B (0.12947)			
10	153A -> 163A (-0.18883) 155A -> 163A (0.11656) 157A -> 163A (-0.11232) 150B -> 162B (-0.17240) 151B -> 162B (-0.17879) 152B -> 162B (-0.37598) 153B -> 162B (0.19014) 155B -> 162B (0.11709) 156B -> 162B (-0.16679) 158B -> 162B (-0.11824) 159B -> 162B (0.415399) 160B -> 162B (-0.29998) 160B -> 164B (0.12153) 161B -> 163B (0.31548) 161B -> 164B (0.36153) 161B -> 165B (0.11013)	2.5614	484.06	0.0062
11	150A -> 163A (-0.23304) 151A -> 163A (-0.13925) 154A -> 163A (-0.21626) 160A -> 163A (-0.29046) 161A -> 163A (0.39886) 162A -> 163A (0.17954)	2.6881	461.24	0.0036

	149B -> 162B (-0.13035) 150B -> 162B (-0.13835) 152B -> 162B (-0.11478) 153B -> 164B (0.14937) 155B -> 162B (0.30039) 156B -> 162B (-0.10559) 156B -> 164B (-0.10725) 159B -> 164B (-0.10704) 160B -> 162B (-0.13238) 160B -> 163B (0.16238) 160B -> 164B (0.27605) 161B -> 164B (-0.17080)			
12	160A -> 164A (0.20912) 161A -> 163A (-0.22136) 162A -> 164A (0.17587) 162A -> 165A (0.12781) 146B -> 162B (-0.15898) 149B -> 162B (-0.27118) 150B -> 162B (-0.17025) 151B -> 162B (0.21880) 155B -> 162B (0.49727) 156B -> 162B (-0.13761) 157B -> 162B (-0.12283) 158B -> 162B (0.16444) 159B -> 163B (0.21152) 160B -> 163B (-0.13723) 160B -> 164B (-0.11602) 161B -> 163B (-0.29895) 161B -> 168B (0.10688)	2.7252	454.95	0.0010
13	154A -> 164A (-0.10250) 160A -> 163A (-0.24711) 160A -> 164A (0.31451) 160A -> 165A (0.11658) 161A -> 164A (0.17552) 161A -> 165A (0.13073) 161A -> 169A (0.11144)	2.7531	450.35	0.0003

	162A -> 164A (0.30579) 162A -> 165A (0.16769) 162A -> 169A (0.12642) 150B -> 162B (0.12297) 153B -> 163B (0.12682) 155B -> 162B (-0.18222) 157B -> 162B (0.23055) 158B -> 162B (-0.15503) 159B -> 163B (0.33546) 159B -> 164B (-0.10325) 159B -> 165B (-0.12344) 160B -> 164B (0.22064) 161B -> 163B (-0.26498) 161B -> 164B (0.29885) 161B -> 165B (0.15165) 161B -> 168B (0.10292)			
14	150A -> 163A (0.11346) 152A -> 163A (0.12180) 153A -> 163A (0.45598) 154A -> 163A (-0.10603) 155A -> 163A (-0.16885) 157A -> 163A (0.16269) 160A -> 163A (0.10535) 160A -> 164A (0.12571) 162A -> 163A (0.13211) 149B -> 162B (0.10133) 152B -> 162B (-0.15857) 152B -> 164B (0.13913) 157B -> 162B (-0.25105) 157B -> 163B (-0.13167) 157B -> 164B (-0.22457) 158B -> 162B (0.10783) 158B -> 163B (-0.15032) 158B -> 164B (-0.21596) 158B -> 170B (0.10715) 159B -> 163B (0.12814)	2.8843	429.87	0.0007

	161B -> 164B (0.19294)			
15	153A -> 163A (0.16474) 162A -> 163A (0.10237) 162A -> 164A (-0.19040) 146B -> 162B (-0.10246) 149B -> 162B (-0.20326) 152B -> 162B (0.22750) 153B -> 162B (0.32507) 154B -> 162B (-0.10522) 156B -> 162B (-0.16534) 157B -> 162B (0.64537) 158B -> 162B (-0.31548)	2.8902	428.98	0.0057
16	160A -> 164A (-0.39796) 160A -> 165A (-0.11095) 162A -> 164A (0.75580) 153B -> 162B (0.10248) 157B -> 162B (0.12564) 159B -> 163B (-0.23705) 159B -> 164B (0.11033) 160B -> 163B (0.28013) 160B -> 164B (-0.14889)	2.9395	421.78	0.0013
17	150A -> 166A (0.24307) 150A -> 167A (-0.11199) 150A -> 173A (0.11191) 152A -> 166A (0.14147) 153A -> 166A (0.29761) 153A -> 167A (-0.12703) 153A -> 173A (0.13917) 155A -> 166A (-0.12386) 157A -> 166A (0.13113) 158A -> 166A (0.10270) 160A -> 166A (0.18468) 161A -> 166A (-0.13811) 162A -> 166A (-0.11058) 152B -> 167B (0.11653) 152B -> 168B (-0.11324)	3.0558	405.74	0.0001

	152B -> 170B (-0.10122) 152B -> 173B (0.12855) 152B -> 174B (-0.16441) 157B -> 167B (-0.13223) 157B -> 168B (0.10259) 157B -> 173B (-0.11908) 157B -> 174B (0.14963) 158B -> 166B (0.13049) 158B -> 167B (-0.21638) 158B -> 168B (0.13436) 158B -> 170B (0.13909) 158B -> 173B (-0.15905) 158B -> 174B (0.21998) 160B -> 166B (0.12404) 160B -> 167B (-0.13916) 160B -> 168B (0.12158) 160B -> 170B (0.13219) 160B -> 173B (-0.12469) 160B -> 174B (0.15727)			
18	149A -> 166A (0.20161) 150A -> 166A (-0.16149) 153A -> 166A (0.22430) 154A -> 166A (-0.17664) 155A -> 166A (-0.15779) 157A -> 166A (0.18803) 160A -> 166A (-0.19492) 161A -> 166A (0.13639) 162A -> 163A (0.10534) 162A -> 166A (0.31862) 162A -> 167A (-0.10122) 162A -> 168A (0.10216) 153B -> 173B (0.10139) 153B -> 174B (-0.12835) 157B -> 166B (0.10294) 157B -> 167B (-0.14795) 157B -> 168B (0.10187)	3.0899	401.26	0.0014

	157B -> 173B (-0.11728) 157B -> 174B (0.14923) 158B -> 166B (0.11053) 158B -> 167B (-0.14604) 158B -> 174B (0.12975) 160B -> 166B (-0.14525) 160B -> 167B (0.11746) 160B -> 168B (-0.11933) 160B -> 173B (0.10286) 160B -> 174B (-0.14931))			
19	160A -> 164A (0.25479) 161A -> 164A (-0.13143) 162A -> 164A (0.45047) 162A -> 165A (-0.19134) 162A -> 166A (-0.10387) 162A -> 167A (0.11424) 162A -> 168A (-0.12765) 159B -> 163B (0.22624) 159B -> 164B (-0.13931) 160B -> 163B (-0.36739) 160B -> 164B (0.15019) 161B -> 163B (0.48149) 161B -> 164B (-0.29169)	3.1701	391.10	0.0112
20	145A -> 163A (0.16459) 150A -> 163A (0.13668) 151A -> 163A (-0.12038) 152A -> 163A (0.14115) 155A -> 163A (0.28443) 156A -> 163A (-0.11053) 157A -> 163A (-0.18129) 160A -> 163A (0.42502) 160A -> 164A (0.10371) 161A -> 163A (0.27555) 161A -> 166A (-0.11452) 162A -> 163A (0.29795) 162A -> 166A (0.11825)	3.1869	389.04	0.0030

151B -> 162B (-0.21734)			
155B -> 162B (0.10899)			
156B -> 162B (0.11294)			
161B -> 165B (0.10318)			

References

- (1) M. Hirotsu, K. Santo, C. Tsuboi and I. Kinoshita, *Organometallics*, 2014, **33**, 4260.
- (2) T. Nakae, M. Hirotsu and I. Kinoshita, *Organometallics*, 2015, **34**, 3988.
- (3) D. W. A. Sharp, *J. Chem. Soc.*, 1957, 4804.
- (4) *CrystalClear*, Rigaku Corporation, 2007.
- (5) L. J. Farrugia, *J. Appl. Crystallogr.* 1999, **32**, 837.
- (6) A. Altomare, M. C. Burla, M. Camalli, G. L. Cascarano, C. Giacovazzo, A. Guagliardi, A. G. G. Moliterni, G. Polidori and R. Spagna, *J. Appl. Crystallogr.* 1999, **32**, 115.
- (7) G. M. Sheldrick, *Acta Cryst.* 2008, **A64**, 112.
- (8) Gaussian 03, Revision E.01, M. J. Frisch, G. W. Trucks, H. B. Schlegel, G. E. Scuseria, M. A. Robb, J. R. Cheeseman, J. A. Montgomery, Jr., T. Vreven, K. N. Kudin, J. C. Burant, J. M. Millam, S. S. Iyengar, J. Tomasi, V. Barone, B. Mennucci, M. Cossi, G. Scalmani, N. Rega, G. A. Petersson, H. Nakatsuji, M. Hada, M. Ehara, K. Toyota, R. Fukuda, J. Hasegawa, M. Ishida, T. Nakajima, Y. Honda, O. Kitao, H. Nakai, M. Klene, X. Li, J. E. Knox, H. P. Hratchian, J. B. Cross, V. Bakken, C. Adamo, J. Jaramillo, R. Gomperts, R. E. Stratmann, O. Yazyev, A. J. Austin, R. Cammi, C. Pomelli, J. W. Ochterski, P. Y. Ayala, K. Morokuma, G. A. Voth, P. Salvador, J. J. Dannenberg, V. G. Zakrzewski, S. Dapprich, A. D. Daniels, M. C. Strain, O. Farkas, D. K. Malick, A. D. Rabuck, K. Raghavachari, J. B. Foresman, J. V. Ortiz, Q. Cui, A. G. Baboul, S. Clifford, J. Cioslowski, B. B. Stefanov, G. Liu, A. Liashenko, P. Piskorz, I. Komaromi, R. L. Martin, D. J. Fox, T. Keith, M. A. Al-Laham, C. Y. Peng, A. Nanayakkara, M. Challacombe, P. M. W. Gill, B. Johnson, W. Chen, M. W. Wong, C. Gonzalez and J. A. Pople, Gaussian, Inc., Wallingford CT, 2004.